Correlation between light absorption and electric charge in solid state electrochromic windows

B.P. JELLE* and G. HAGEN
Department of Electrochemistry, Norwegian University of Science and Technology (NTNU), N-7034 Trondheim, Norway
(*author for correspondence)

Abstract

Electrochromic windows based on different combinations of the electrochromic materials polyaniline (PANI), Prussian Blue (PB) and tungsten oxide (WO_3), with the solid state polymer electrolyte poly(2-acrylamido-2-methyl-propane-sulphonic acid) (PAMPS) as an ionic conductor, have been studied. These windows show a large transmission regulation both in the visible and in the near infrared wavelength region. Integrated over the solar spectrum, wind\ws with PB deposited on top of PANI, with WO_3 as a complementary coating, are typically able to regulate as much as 50% of the total solar radiation. The relationship between light absorption and charge extraction in electrochromic windows has been studied. The windows are coloured by applying a potential, which is then switched off, and the discharge process is followed by continuously measuring the light absorption and the charge extraction through a connected resistor. From the resulting linear relationship between the absorption and charge extraction, the overall absorption coefficient may be calculated.

1. Introduction

Dynamic sun radiation control in windows may be achieved by use of electrochromic windows, called 'smart windows' [1–3], which change colour with applied voltage. It is essential to regulate the whole solar spectrum (300–3000 nm), that is, both the ultraviolet (u.v., 300–400 nm), the visible (vis., 400–700 nm) and the near infrared (n.i.r., 700–3000 nm) region should be sufficiently regulable. It should be noted that almost half of the solar energy lies in the n.i.r. region [2–7].

Commercial applications of electrochromic materials already exist in the form of car mirrors (e.g., Gentex [8]), and the following years will probably extend these applications to larger areas such as sun roofs in cars and windows in buildings. Electrochromic windows may easily handle seasonal fluctuations, For example, let sunlight into the buildings during winter and shut off sunlight from entering the buildings during summer. Visible colour changes may also be exploited in an architectural way (i.e.,'fancy windows' [9]).

With electrochromic windows based on polyaniline (PANI), Prussian Blue (PB) and tungsten oxide (WO_3) we have been able to typically regulate as much as 50% of the total solar energy [9–11]. In this work we are investigating the relationship between light absorption and electric charge extraction in these windows.

2. Experimental details

Two electrochromic windows, denoted D1 (PANI‖ WO_3) and D2 (PANI|PB‖WO_3), which may be written on the sandwich form as glass|ITO|PANI|PAMPS| WO_3|ITO|glass and glass|ITO|PANI|PB|PAMPS|WO_3| ITO|glass, respectively, have been fabricated. PAMPS denotes the solid polymer electrolyte poly(2-acrylamido-2-methyl-propane-sulphonic acid) and ITO denotes the transparent conductor indium-tin oxide. D1 and D2 are identical except for the PB layer in D2.

The polyaniline films were deposited electrochemically at a constant current of 0.015 mA cm^{-2} for 2000 s on ITO glass plates (90 Ω $\square^{-1}$) from aqueous solutions of aniline in sulphuric acid (0.02 M aniline and 0.5 M H_2SO_4). The Prussian Blue film was thereafter deposited onto one of the PANI coatings (for D2) by applying a constant current of −0.0031 mA cm^{-2} for 1500 s in an electrolyte consisting of 0.5 M $KHSO_4$, 0.001 M $K_3[Fe(CN)_6]$ and 0.001 M $Fe_2(SO_4)_3$. The electrolyte for the tungsten oxide formation was prepared by dissolving 4.52 g of tungsten in 60 ml 30% hydrogen peroxide, and diluting with distilled water to a total volume of 500 ml, thus giving a tungsten concentration of 0.049 M. The WO_3 films were formed on ITO glass plates by applying a constant potential of −700 mV vs. Ag/AgCl (3.0 M KCl) for 300 s. Before further use, the WO_3 films were heated at 140 °C for

1 h. Platinum was used as a counter electrode for the electrodepositions of PANI, PB and WO$_3$ layers, while Ag/AgCl (3.0 M KCl) was applied as a reference electrode.

The electrochromic electrodes (PANI and WO$_3$, PANI|PB and WO$_3$) for the two device configurations were glued together with the solid polymer electrolyte PAMPS after a procedure described elsewhere [12], and sealed with epoxy. The electrochromic device area was 1.0 cm $\times$ 3.1 cm (3.1 cm^2). It should be noted that our electrochromic windows are small laboratory windows, while a real window at full scale requires either application of higher voltages or better conducting transparent electrodes. Higher voltages may degrade the electrochromic materials and the transparent conductor at the window edges. Better conducting transparent electrodes implies a higher transparent coating conductivity or a highly conducting grid (e.g., thin copper wires) in combination with the transparent coating. These considerations may help eliminate problems with inhomogeneous electrochromic layers and slow gradually colour changes over large window surfaces, for the electrochemical depositions and the operation of the windows, respectively. The PANI, PB and WO$_3$ films were each less than 1 μm thick, while the PAMPS layer was about 0.1 mm. A schematic drawing of the device configurations with and without PB is shown in Figure 1, with electrode reactions as described elsewhere [9].

An AutoLab PGSTAT20 potentiostat/galvanostat/ frequency response analyser was used in the electrochemical deposition of PANI, PB and WO$_3$ films, and in the impedance measurements. The transmission experiments were carried out with a Cary 5 u.v–vis.–n.i.r spectrophotometer in the 290–3300 nm wavelength region. Before recording the transmission spectra a constant potential was applied for several minutes (sometimes hours) with a Gerhard Bank Elektronik Göttingen potentiostat MP81 to stabilize the colour changing films. The potential was also applied during the wavelength scan. Applying a positive potential to the PANI or the PANI|PB electrode, both PANI, PB and WO$_3$ turned to a blue colour, while the window was bleached (made almost transparent) by reversing the polarity of the electrodes.

The experimental set-up for measuring light absorption and voltage with time during discharging through different resistors (1.2 Ω–21 MΩ, open circuit) is shown in Figure 2. A computer interfaced Solartron Schlumberger 7150 Plus digital multimeter was used to measure the voltage during the discharging. A light beam with intensity I_0 (at a wavelength of 600 nm) is sent through the sample (i.e., PANI, PB, WO$_3$) of thickness x. The windows are coloured by applying a potential, which is then switched off, and the discharge process is followed by continuously measuring the light absorption, A', and the voltage, U, over a connected
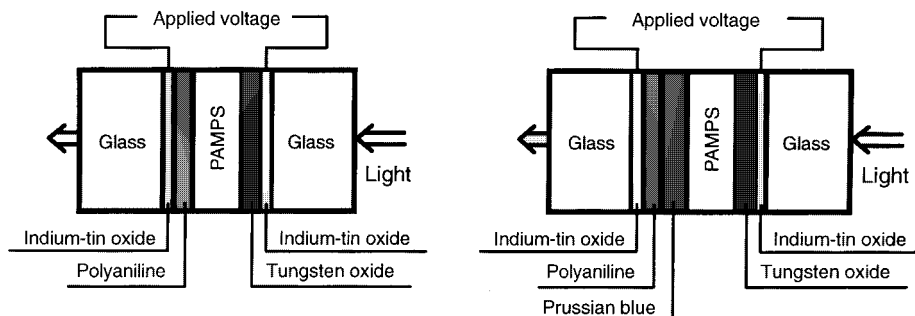

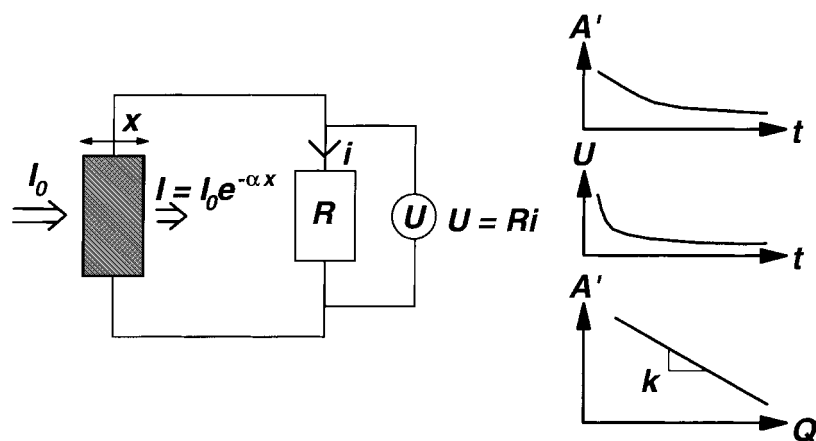Fig. 1. Schematic drawings of the ECW configurations without PB (D1) and with PB (D2).

Fig. 2. Experimental setup for measuring light absorption and voltage with time during discharging through different resistors and open circuit. Linear relationship between light absorption and charge extraction is depicted.

resistor. The charge extraction, Q, is calculated from the current, i, through the resistor, R, applying Ohm's law integrating over the time, t. From the Beer–Lambert law and the resulting linear relationship between the absorption and charge extraction, the absorption coefficient α may be calculated. Further details are given in the following Section.

3. Results and discussion

The measured transmission spectra in the 290–3300 nm wavelength region for the two electrochromic windows D1 (without PB) and D2 (with PB) are given in Figure 3, showing a large transmission modulation, especially for D2. The applied potentials are listed from top to bottom in the figures, corresponding to a decreasing order of the transmission spectra. Employing a calculation procedure described elsewhere [9–10], it is found that the total solar energy regulation is 41% for the window based on PANI and WO_3 (D1), while the inclusion of PB (D2) yields a total solar energy modulation of 53% [11]. As with most of the work on electrochromic windows so far, it should be noted that also these windows are radiation absorbing, rather than radiation reflecting. Reflection modulation is generally being preferred for several reasons [13–19]: (i) absorbing window panes may become unacceptable hot, which may lead to degradation of the different layers, (ii) absorbing modulating windows have lower thermal transfer efficiency, (iii) absorption modulation requires thicker films than reflection modulation, leading to higher manufacturing and operation costs, and (iv) spectrally selective modulation (filtering) is believed to be more readily achieved by reflection regulation (free charge carrier density and dynamics) than by bound electron absorption modulation. Besides, especially polymers (e.g., PANI) are considered to be sensitive to u.v. radiation, although this degradation risk is lowered by the u.v. absorption in the glass panes.

Long time memory experiments for D1 and D2 are depicted in Figure 4. The windows were kept on the shelf with no attachments to the electrodes during and between the measurements (i.e. true open circuit). The memory in the transparent state was measured up to seven days, and showed only a small transmission change in the n.i.r. region, while the transmission in the u.v.–vis. region was almost identical after seven days, for both D1 and D2. In the coloured state the memory was not so stable as in the transparent state, but nevertheless the windows retained a substantial colouration for 1–7 days, and even after 176 days there is still some memory left, for both D1 and D2. All these long time memory measurements (Figure 4) were carried out before the subsequent experiments depicted in Figures 5–13, which is important to note as we during the
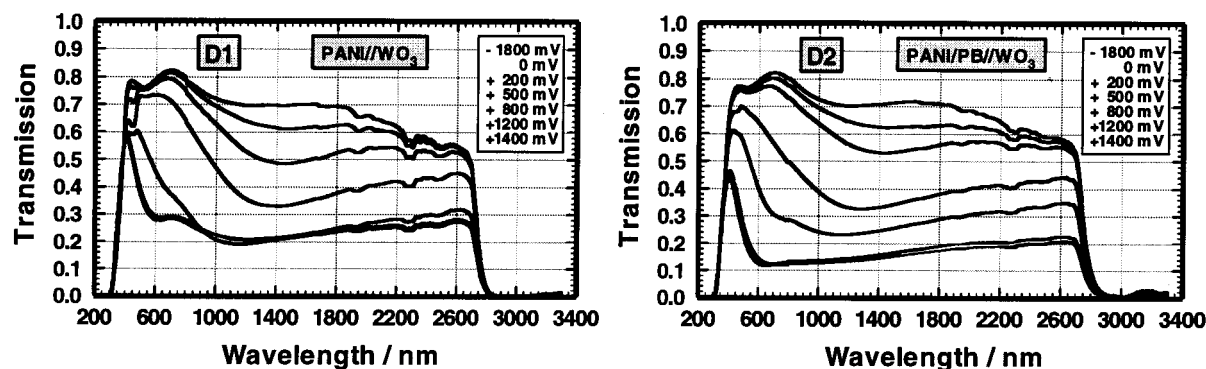

Fig. 3. Transmission against wavelength for electrochromic windows D1 and D2 at different applied potentials. Total solar energy regulations are 41% and 53%, respectively [11].
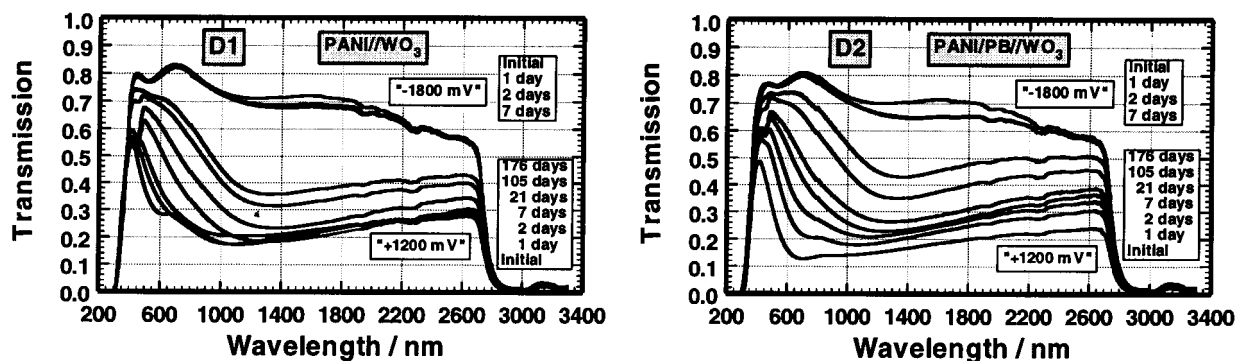

Fig. 4. Transmission against wavelength for different times of measurement after switching off the potential.
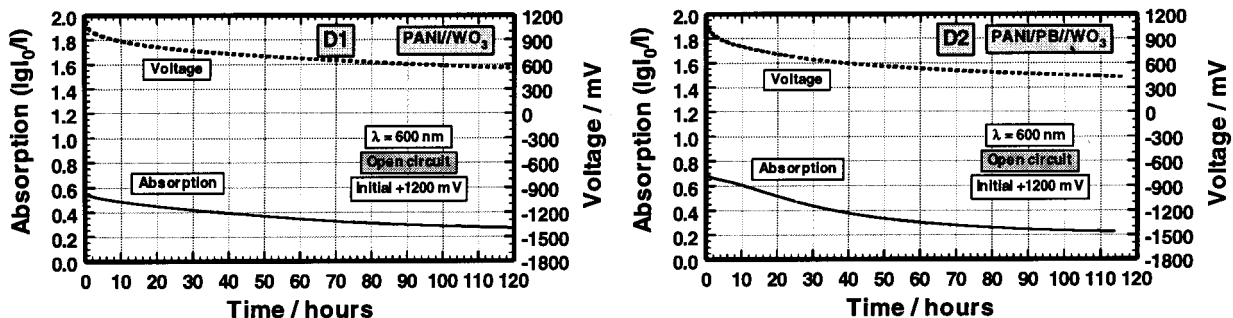
Fig. 5. Absorption (at 600 nm) and voltage against time (up to five days) for the open circuit condition for D1 and D2.

discharge experiments (Figures 5–13) probably experienced an internal short circuit in the D2 window, resulting in irreversible changes (further discussed below).

With an experimental setup as shown in Figure 2 the light absorption (at 600 nm) and voltage were measured with time during discharging through different resistors and at open circuit. In Figure 5 the absorption and voltage in the open circuit case (multimeter connected, input resistance >10 GΩ in the actual voltage range) were measured up to five days, showing a gradually absorption and voltage decrease for both D1 and D2. After five days potentials of 400–600 mV were still obtained (from initially 1200 mV).

Two examples of the absorption (at 600 nm) and voltage measured with time (up to 5 h) during discharge through resistors of 3 kΩ and 1 MΩ for D1 are shown in Figure 6, while the similar plots for the other resistors in the whole resistor range 1.2 Ω–21 MΩ and open circuit

are not depicted here. Correspondingly, the absorption/voltage vs. time measurements for D2 are shown in Figure 7. Naturally, both the absorption and the voltage decrease during the discharge through resistors, for both D1 and D2. For D1 and resistors between 1.2 Ω–10 kΩ the voltage drops rapidly close to zero, while between 100 kΩ–21 MΩ – open circuit, the voltage decreases substantially more slowly with increasing resistance. For D1 and resistors between 1 MΩ–21 MΩ – open circuit the absorption decrease significantly more slowly. Unfortunately, during the experiments D2 changed behaviour in the way that the voltage drops rapidly close to zero even for large resistors and open circuit. Besides, the absorption decrease for large resistors and open circuit is more or less the same as for low resistor values. In addition, the absorption is lower at an applied potential of +1200 mV than it normally should be. This is probably due to an internal short circuit in the D2 window. The results for D2 may therefore not be
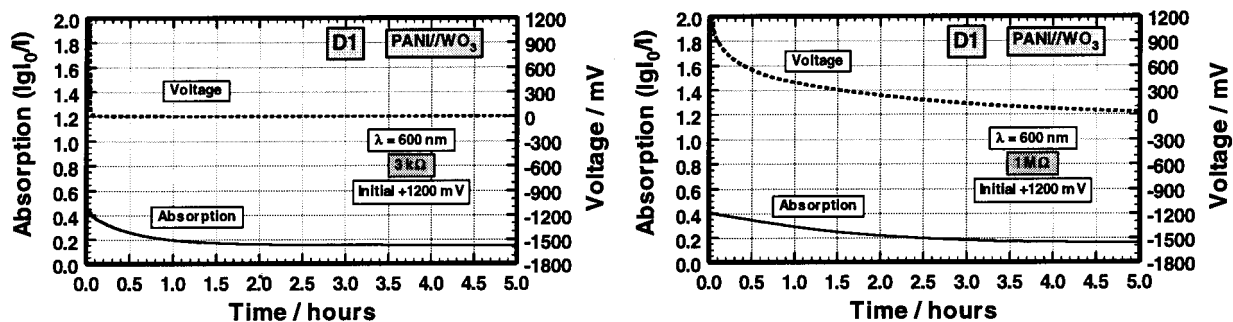

Fig. 6. Absorption (at 600 nm) and voltage against time for resistors of 3 kΩ and 1 MΩ for D1.
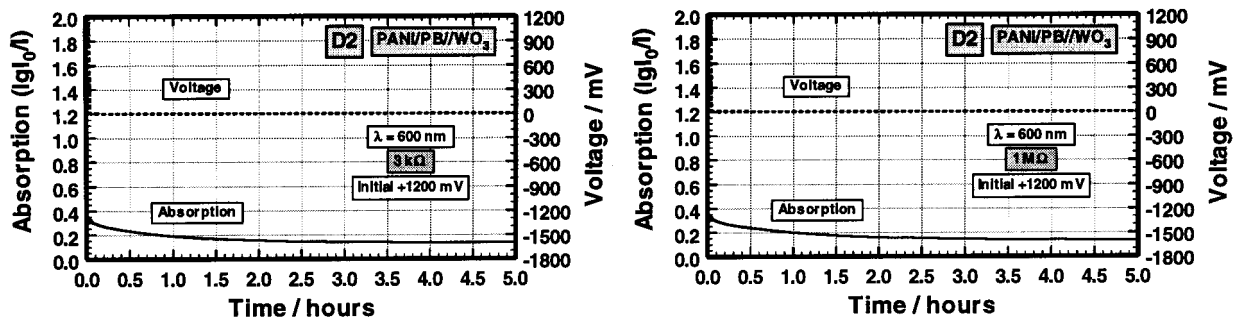

Fig. 7. Absorption (at 600 nm) and voltage against time for resistors of 3 kΩ and 1 MΩ for D2.

directly compared to D1. However, as will be shown in the following for D2, there is a linear relationship between absorption and charge for all resistor values except 1.2 Ω, absorption coefficients may still be estimated, and for low resistor values an electrochromic efficiency may be calculated.

The relationship between light absorption and charge extraction was investigated. Based on the data from Figure 6 the absorption is plotted vs. the charge extraction for D1 in Figure 8, yielding an approximately linear relationship except for the smallest resistor of 1.2 Ω. Correspondingly, from Figure 7 a linear relationship is plotted in Figure 9 (except for 1.2 Ω) for D2. The deviation from linearity at 1.2 Ω may be explained from the fact that in the case of almost electrical short circuit, the absorption change may not be so fast in relationship to the voltage drop, compared to absorption/voltage relationships at larger resistors.

The measured absorption A', or optical density (OD), is written on the logarithmic form

$$A' = OD = \log_{10}(1/T) = \log_{10}(I_0/I) = \lg(I_0/I) \qquad (1)$$

where T denotes the transmission, I_0 the incident light intensity and I the transmitted light intensity (from the sample, i.e., window). From the well-known Beer–Lambert law (see Fig. 2)

$$I = I_0 e^{-\alpha x} \qquad (2)$$

one may write Equation 1 as

$$A' = (\alpha \lg e)x = \alpha'x \qquad (3)$$

where α denotes the absorption coefficient and x the sample thickness (i.e., PANI, PB, WO$_3$). Assuming, which is supported by the measurements (Figs. 8 and 9), that the absorption change is proportional to the charge extraction (or injection), that is,

$$A' = \alpha'x = kQ = k \int i(t)\, dt \qquad (4)$$

the absorption coefficient may be calculated from

$$\alpha = A'/(x \lg e) = kQ/(x \lg e) = \frac{k \int i(t)\, dt}{x \lg e} \approx \frac{k \int i(t)\, dt}{0.434\, x} \qquad (5)$$

where the correlation slope k is found from Figures 8 and 9 (and similar plots for the whole resistor range), and the charge extraction Q is calculated by integrating the current $i(t)$ (given by Ohm's law; $U = Ri$, where U and R denote the voltage and resistance, respectively) over the time t. Based partly on earlier measurements of PANI and WO$_3$ coating thicknesses, PANI and PB are each assumed to be 50 nm in thickness, while WO$_3$ is assumed to be 400 nm.
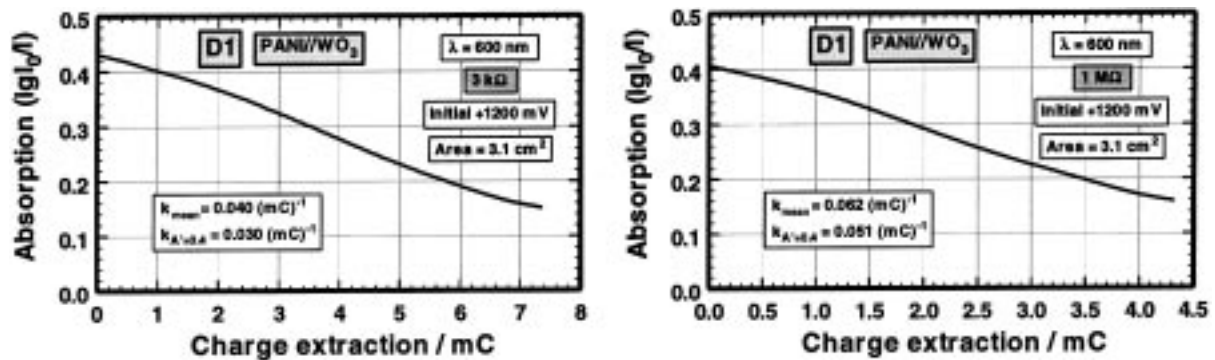

Fig. 8. Absorption against charge extraction for resistors of 3 kΩ and 1 MΩ for D1.
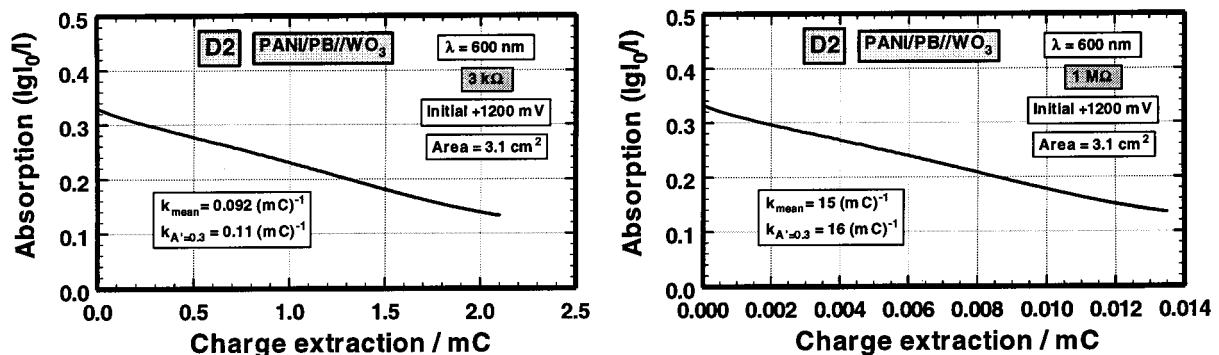

Fig. 9. Absorption against charge extraction for resistors of 3 kΩ and 1 MΩ for D2.

Table 1. Corresponding k and α values for different resistors for the electrochromic window D1 (Figs 2 and 8)
Electrochromic area 3.1 cm^2. Assumed: PANI = 50 nm and WO$_3$ = 400 nm

Resistor /Ω	k_{mean} /(mC)$^{-1}$	$k_{A'=0.4}$ /(mC)$^{-1}$	α_{mean} /10^6 m^{-1}	$\alpha_{A'=0.4}$ /10^6 m^{-1}
1.2	–	0.038	–	4.3
10	0.033	0.041	1.5	1.9
100	0.041	0.036	1.4	1.2
300	0.040	0.032	1.4	1.1
1×10^3	0.048	0.038	1.2	0.96
3×10^3	0.040	0.030	1.5	1.1
10×10^3	0.039	0.042	1.5	1.6
100×10^3	0.036	0.036	1.5	1.5
1×10^6	0.062	0.051	1.4	1.1
11×10^6	0.41	0.29	1.3	0.91
21×10^6	0.21	0.22	0.67	0.70
Average*	0.040	0.036	1.4	1.3

* For resistor values between 10 Ω–100 kΩ and 10 Ω–11 MΩ for k and α, respectively

Table 2. Corresponding k and α values for different resistors for the electrochromic window D2 (Figs 2 and 9)
Electrochromic area 3.1 cm^2. Assumed: PANI = 50 nm, PB = 50 nm and WO$_3$ = 400 nm

Resistor /Ω	k_{mean} /(mC)$^{-1}$	$k_{A'=0.3}$ /(mC)$^{-1}$	α_{mean} /10^6 m^{-1}	$\alpha_{A'=0.3}$ /10^6 m^{-1}
1.2	–	0.014	–	3.6
10	0.035	0.047	1.0	1.4
100	0.047	0.047	0.97	0.97
300	0.053	0.056	0.93	0.98
1×10^3	0.079	0.079	1.1	1.1
3×10^3	0.092	0.11	0.89	1.1
10×10^3	0.19	0.23	0.95	1.1
100×10^3	0.99	0.99	1.1	1.1
1×10^6	15	16	0.93	0.99
11×10^6	140	140	1.0	1.0
21×10^6	260	260	1.0	1.0
Average*	0.045	0.050	0.99	1.1

* For resistor values between 10 Ω–300 Ω and 10 Ω–21 MΩ for k and α, respectively

The calculated k and α values are given in Tables 1 and 2, for D1 and D2, respectively. The k_{mean} and α_{mean} values are calculated from the mean correlation slope k for each resistor in Figures 8 and 9 (and the whole resistor range). The $k_{A'=0.4}(k_{A'=0.3})$ and $\alpha_{A'=0.4}(\alpha_{A'=0.3})$ values are calculated from the tangent correlation slope k at an absorption value of 0.4 for D1 (0.3 for D2) for each resistor in Figures 8 and 9 (and the whole resistor range). Applying this tangent correlation slope at one certain absorption value may contribute to ensure that the electrochromic window is in the same state for the calculations.

The k values for D1 are of the same order for resistors between 10 Ω–100 kΩ, while for larger resistors the k values are increasing somewhat, which may indicate that some kind of relaxation processes are becoming more dominant at lower discharging (larger resistors). Furthermore, the long time memory experiments at open circuit in Figure 4 (and Figure 5) indicate that relaxation processes, with decreasing absorption as a result, take place. For D1 the average values are found to be: $k_{mean} = 0.040$ (mC)$^{-1}$, $k_{A'=0.4} = 0.036$ (mC)$^{-1}$, $\alpha_{mean} = 1.4 \times 10^6$ m^{-1} and $\alpha_{A'=0.4} = 1.3 \times 10^6$ m^{-1}. The k values for D2 increases more or less steadily for the whole

resistor range (an average value may only be taken between 10 Ω–300 Ω), which is probably due to some unknown internal short circuit in the D2 window. An internal short circuit will lead to decreasing discharge through the resistors with increasing resistor values, and with approximately the same absorption change this will result in higher correlation slope values ($k = A'/Q$, Equation 4). However, the calculation of the α values is not influenced by the increasing k values since the decreasing charge extraction is compensated by the multiplication with the charge in the expression for α (Equation 5). For D2 the average values are found to be: $k_{mean} = 0.045$ (mC)$^{-1}$, $k_{A'=0.3} = 0.050$ (mC)$^{-1}$, $\alpha_{mean} = 0.99 \times 10^6$ m^{-1} and $\alpha_{A'=0.3} = 1.1 \times 10^6$ m^{-1} (the k values are taken only between 10 Ω–300 Ω). With no internal short circuit in D2 the absorption coefficients would have been larger as the absorption changes would also have been larger (e.g., Equation 5). A visualization of some of the results in Tables 1 and 2 is given in Figures 10 and 11, showing the correlation slope k and the absorption coefficient α for different applied resistors (for both D1 and D2).

The electrochromic efficiency η is defined as the absorption change A' (or $\Delta A'$) divided by the consumed
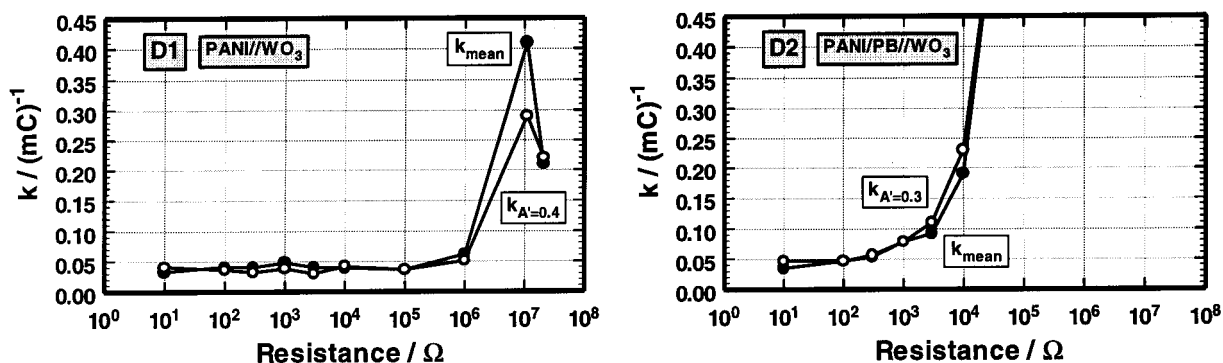

Fig. 10. Correlation slope k between absorption and charge plotted against applied resistors for the electrochromic windows D1 and D2.
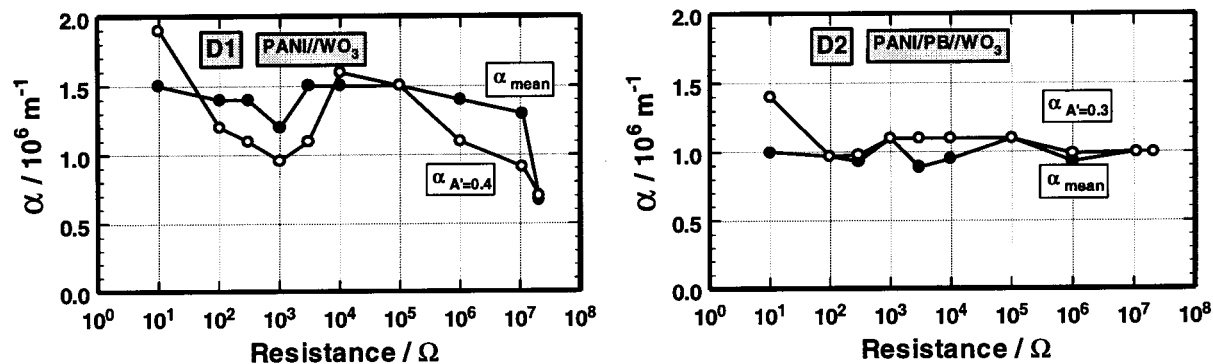
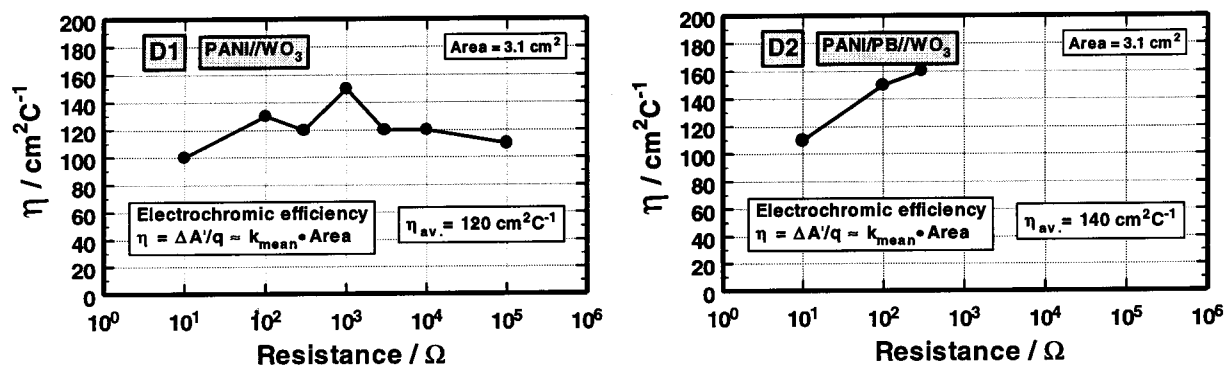Fig. 11. Absorption coefficient α plotted against applied resistors for the electrochromic windows D1 and D2.

Fig. 12. Electrochromic efficiency at 600 nm calculated as the product of k_{mean} and the electrochromic window area in the resistor range 10 Ω–100 kΩ and 10 Ω–300 Ω for D1 and D2, respectively.

charge density, q, and is here found from multiplying the correlation slope, k, with the actual electrochromic area (3.1 cm²) as follows:

$$\eta = \Delta A'/q = \Delta A' \times \text{Area}/Q = k_{mean} \times \text{Area} \qquad (6)$$

The average electrochromic efficiencies (bleaching efficiencies in these cases, at 600 nm) as depicted in Figure 12 are calculated to 120 cm² C⁻¹ for D1 and 140 cm² C⁻¹ for D2 (for resistor ranges 10 Ω–100 kΩ and 10 Ω–300 Ω, respectively). These values may be compared to a bleaching efficiency of 120 cm² C⁻¹ (at 550 nm) reported earlier from potential step experiments for a PANI, PB and WO₃ based window [20].

The electrochemical impedance for D1 and D2 shown in Figure 13 was measured at applied potentials of −1800 mV and +1200 mV, and for different times (from minutes to days) after switching off the applied potential. It is seen that the impedance increases from the coloured state (+1200 mV) to the transparent state (−1800 mV) for both D1 and D2, for example, by switching off the potential of +1200 mV the impedance
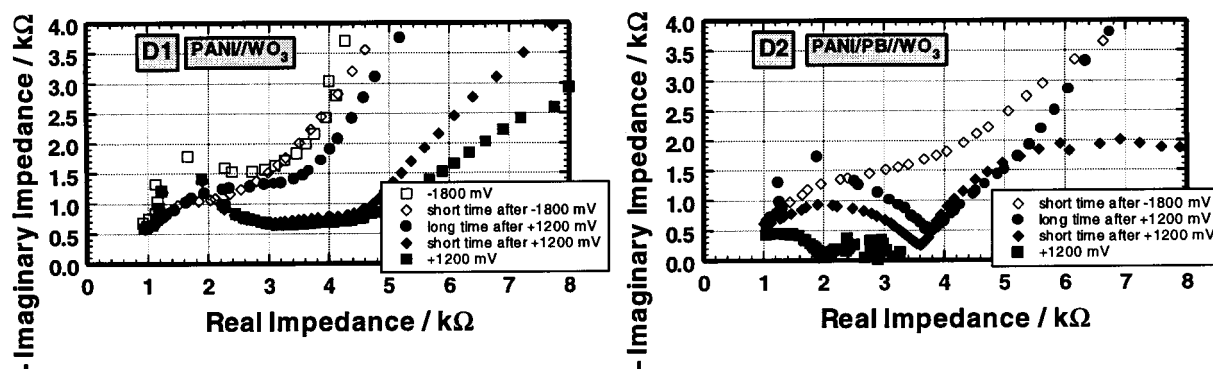

Fig. 13. Impedance spectra for D1 and D2 measured at potentials of −1800 mV and +1200 mV, and for different times after switching off the applied potential. Short and long time denote some minutes and 5 days, respectively. Area 3.1 cm². Measured frequency range 50 kHz–10 mHz (10 points/decade) with a sinusoidal amplitude of 5 mV. Frequency range (in figure): 50 kHz to 390 Hz (−1800 mV), 260 Hz (short time after −1800 mV), 200 Hz (long time after +1200 mV), 0.98 Hz (short time after +1200 mV) and 0.60 Hz (+1200 mV) for D1 and 50 kHz to 160 Hz (short time after −1800 mV), 4.2 Hz (long time after +1200 mV), 0.23 Hz (short time after +1200 mV) and 0.01 Hz (+1200 mV) for D2.

is gradually increasing and approaching at long times the impedance spectra for the transparent state. Impedance spectroscopy is strictly only valid for steady state, which is clearly not the case here. To attempt to utilize impedance spectroscopy in connection with the correlation between absorption and charge, one should perform relative fast frequency scans taking less time than the timescale for significant changes in the system (i.e., relative high frequencies may be necessary).

These electrochromic windows with two (D1) and even three (D2) electrochromic layers, and where the doping mechanisms in PANI include both redox processes and proton doping [21–23], are complicated systems where several reactions may take place. This is indicated in Figures 8 and 9 where the relationship between the light absorption and the electric charge is not completely linear. It might be worth the effort to investigate this further, for example, in connection with the earlier presented '*hole method*' [11], although this method has limitations in kinetic measurements.

4. Conclusions

High solar transmission modulation was achieved for the electrochromic windows. The window based on polyaniline (PANI) and tungsten oxide (WO_3) (abbreviated $PANI\|WO_3$) regulates 41%, while the window based on polyaniline (PANI), Prussian Blue (PB) and tungsten oxide (WO_3) (abbreviated $PANI|PB\|WO_3$) regulates as much as 53% of the total solar energy.

The electrochromic windows $PANI\|WO_3$ and $PANI|PB\|WO_3$ have demonstrated satisfactory memory effects. The memory is quite good in both the bleached and coloured state for 1–7 days, and there is still some memory left in the coloured state after 176 days.

Light absorption and voltage were measured against time during discharging through different resistors. A linear relationship between absorption and charge extraction was found, allowing calculation of absorption coefficients, $\sim 1.4 \times 10^6 \, m^{-1}$ for $PANI\|WO_3$ and $\sim 1.0 \times 10^6 \, m^{-1}$ for $PANI|PB\|WO_3$. Electrochromic efficiencies were also calculated from these linear relationships, $120 \, cm^2 \, C^{-1}$ and $140 \, cm^2 \, C^{-1}$ for $PANI\|WO_3$ and $PANI|PB\|WO_3$, respectively.

Acknowledgements

References

1. J.S.E.M. Svensson and C.G. Granqvist, *Appl. Phys. Lett.* **45** (1984) 828.
2. J.S.E.M. Svensson and C.G. Granqvist, *in* 'Optical Materials Technology for Energy Efficiency and Solar Energy Conversion III' (edited by C.M. Lampert), The Society of Photo-Optical Instrumentation Engineers, Bellingham, Washington, *Proc. SPIE – Int. Soc. Opt. Eng.* **502** (1984) 30.
3. J.S.E.M. Svensson and C.G. Granqvist, *Sol. Energy Mater.* **12** (1985) 391.
4. C.G. Granqvist, *The Physics Teacher* **22** (Sept. 1984) 372.
5. C.G. Granqvist, *in* 'Window Industries' (edited by P. de Lacey), (Turret-Wheatland, Aug. 1987), pp. 22–24.
6. C.G. Granqvist, *in* 'Electricity. Efficient End-use and New Generation Technologies, and their Planning Implications' (edited by T.B. Johansson, B. Bodlund and R.H. Williams), (Lund University Press, 1989), pp. 89–123.
7. C.G. Granqvist, *in* 'Material Science for Solar Energy Conversion Systems' (edited by C.G. Granqvist), (Pergamon Press, 1991), pp. 106–167.
8. www.gentex.com/automotive/nvs.htm (1998).
9. B.P. Jelle and G. Hagen, *J. Electrochem. Soc.* **140** (1993) 3560.
10. B.P. Jelle, G. Hagen and S.Nødland, *Electrochim. Acta* **38** (1993) 1497.
11. B.P. Jelle, G. Hagen and Ø. Birketveit, *J. Appl. Electrochem.* **28** (1998) 483.
12. B.P. Jelle, G. Hagen and R. Ødegård, *Electrochim. Acta* **37** (1992) 1377.
13. R.B. Goldner and R.D. Rauh, *Sol. Energy Mater.* **11** (1984) 177.
14. R.B. Goldner, A. Brofos, G. Foley, E.L. Goldner, T.E. Haas, W. Henderson, P. Norton, B.A. Ratnam, N. Weis and K.K. Wong, *Sol. Energy Mater.* **12** (1985) 403.
15. R.B. Goldner, K. Wong, G. Foley, P. Norton, L. Wamboldt, G. Seward, T. Haas and R. Chapman, *Sol. Energy Mater.* **16** (1987) 365.
16. R.B. Goldner, T.E. Haas, G. Seward, K.K. Wong, P. Norton, G. Foley, G. Berera, G. Wei, S. Schulz and R. Chapman, *Solid State Ionics* **28–30** (1988) 1715.
17. R.B. Goldner, G. Seward, K. Wong, T. Haas, G.H. Foley, R. Chapman and S. Schulz, *Sol. Energy Mater.* **19** (1989) 17.
18. R.B. Goldner, G. Berera, F.O. Arntz, T.E. Haas, B. Morel and K.K. Wong, *in* 'Electrochromic Materials' (edited by M.K. Carpenter and D.A. Corrigan), Proceedings of the Symposium on Electrochromic Materials, The 176th Meeting of The Electrochemical Society, Hollywood, FA, 16–18 Oct. 1989, The Electrochemical Society, Pennington, NJ, **PV 90-2** (1990) 14.
19. R.B. Goldner, F.O. Arntz, G. Berera, T.E. Haas, G. Wei, K.K. Wong and P.C. Yu, *Solid State Ionics* **53–56** (1992) 617.
20. B.P. Jelle and G. Hagen, *in* 'Electrochromic Materials II' (edited by K.C. Ho and D.A. MacArthur), Proceedings of the Symposium on Electrochromic Materials, The 184th Meeting of The Electrochemical Society, New Orleans, LA, 10–15 Oct. 1993, The Electrochemical Society, Pennington, NJ, **PV 94-2** (1994) 324.
21. W.S. Huang, B.D. Humphrey and A.G. MacDiarmid, *J. Chem. Soc., Faraday Trans. 1* **82** (1986) 2385.
22. J.C. Chiang and A.G. MacDiarmid, *Synth. Met.* **13** (1986) 193.
23. B.P. Jelle, G. Hagen, S.M. Hesjevik and R. Ødegård, *Electrochim. Acta* **38** (1993) 1643.